iJRASET
International Journal For Research in Applied Science and Engineering Technology

INTERNATIONAL JOURNAL FOR RESEARCH

IN APPLIED SCIENCE & ENGINEERING TECHNOLOGY

Volume: 14 **Issue:** VI **Month of publication:** June 2026

DOI: https://doi.org/10.22214/ijraset.2026.83724

www.ijraset.com

Call: 08813907089 | E-mail ID: ijraset@gmail.com

International Journal for Research in Applied Science & Engineering Technology (IJRASET)
ISSN: 2321-9653; IC Value: 45.98; SJ Impact Factor: 7.538
Volume 14 Issue VI June 2026- Available at www.ijraset.com

Structural, Thermal and Upconversion Properties of Pr^{3+} doped Borosilicate Glasses for Display Device Applications

S. L. Meena
Ceramic Laboratory, Department of physics, Jai Narain Vyas University, Jodhpur 342001(Raj.) Ind

Abstract: ***Yttrium zinc lithium alumino antimony sodalime borosilicate glasses containing Pr^{3+} in (20-x):SiO_2:10ZnO: 10Li_2O :10Al_2O_3 :10Sb_2O_3 :10Na_2O :10CaO :10Y_2O_3 :10B_2O_3:xPr_2O_3 (where x=1, 1.5,2 mol %) have been prepared by melt-quenching method. The amorphous nature of the glasses was confirmed by x-ray diffraction studies. DTA curve was analysed to evaluate the glass transition temperature, crystallization temperature and melting temperature. Optical absorption, Excitation spectra and fluorescence spectra were recorded at room temperature for all glass samples. Judd-Ofelt intensity parameters Ω_λ (λ=2, 4, 6) are evaluated from the intensities of various absorption bands of optical absorption spectra. Using these intensity parameters various radiative properties like spontaneous emission probability, branching ratio, radiative life time and stimulated emission cross–section of various emission lines have been evaluated.***

Keywords: YZLAASLBS Glasses, Optical Properties, Judd-Ofelt Theory, Thermal Properties.

I. INTRODUCTION

Rare earth doped ceramic glasses as host materials for active optical ions have attracted great interest recently due to their potential application in optical fiber amplifiers, frequency-conversion materials, lasers and optical devices [1–5]. Silicate glasses have large transparency, low phonon energy, good thermal stability, high refractive index, high density, good mechanical, optical and chemical properties [6-10]. Silicate glasses are very important because of the possibility of their application in optoelectronic, optic device fields, such as lasers, fiber optic large bandwidth, absorption cross-section and solar cells and high emission. The addition of network modifier (NWF) Li_2O is to improve both mechanical electrical and electrical properties[11-14]. Recently, rare earth doped silicate glass has attracted much interest because of high rare earth ion solubility, optical data transmission, detection, sensor and catalysts [15-18].

In this work, the spectroscopic properties of Pr^{3+} -doped (20-x):SiO_2:10ZnO :10Li_2O :10Al_2O_3 :10Sb_2O_3 :10Na_2O :10CaO :10Y_2O_3 :10B_2O_3:xPr_2O_3 (where x=1, 1.5,2 mol %) glasses were investigated. absorption, Excitation spectra and fluorescence spectra, The DTA, absorption, Excitation and fluorescence spectra of Pr^{3+} of the glasses were investigated. The J-O intensity parameters render significant information regarding local structure and bonding in the vicinity of rare- earth ions.

II. EXPERIMENTAL TECHNIQUES

A. Preparation of Glasses

The following Pr^{3+} doped yttrium zinc lithium alumino antimony sodalime borosilicate glass samples (20-x):SiO_2:10ZnO :10Li_2O :10Al_2O_3 :10Sb_2O_3 :10Na_2O :10CaO :10Y_2O_3 :10B_2O_3:xPr_2O_3 (where x=1, 1.5.2) have been prepared by melt-quenching method. Analytical reagent grade chemical used in the present study consist of SiO_2, ZnO, Li_2O,Al_2O_3,Sb_2O_3,Na_2O,CaO,Y_2O_3, B_2O_3 and Pr_2O_3. All weighed chemicals were powdered by using an Agate pestle mortar and mixed thoroughly before each batch (10g) was melted in alumina crucibles in silicon carbide based an electrical furnace.

Silicon Carbide Muffle furnace was heated to working temperature of 1050^0C, for preparation of yttrium zinc lithium alumino antimony sodalime borosilicate glasses, for two hours to ensure the melt to be free from gases. The melt was stirred several times to ensure homogeneity. For quenching, the melt was quickly poured on the steel plate & was immediately inserted in the muffle furnace for annealing. The steel plate was preheated to100^0C.While pouring; the temperature of crucible was also maintained to prevent crystallization. And annealed at temperature of 350^0C for 2h to remove thermal strains and stresses. Every time fine powder of cerium oxide was used for polishing the samples. The glass samples so prepared were of good optical quality and were transparent. The chemical compositions of the glasses with the name of samples are summarized in Table 1

Table 1 Chemical composition of the glasses

Sample	Glass composition (mol %)
YZLAASLBS (UD)	$20SiO_2$:10ZnO :$10Li_2O$:$10Al_2O_3$:$10Sb_2O_3$:$10Na_2O$:10CaO :$10Y_2O_3$:$10B_2O_3$
YZLAASLBS PR(1.0)	19 SiO_2:10ZnO :$10Li_2O$:$10Al_2O_3$:$10Sb_2O_3$:$10Na_2O$:10CaO :$10Y_2O_3$:$10B_2O_3$:1 Pr_2O_3
YZLAASLBS PR (1.5)	18.5SiO_2:10ZnO :$10Li_2O$:$10Al_2O_3$:$10Sb_2O_3$:$10Na_2O$:10CaO :$10Y_2O_3$:$10B_2O_3$:1.5 Pr_2O_3
YZLAASLBS PR(2.0)	$18SiO_2$:10ZnO :$10Li_2O$:$10Al_2O_3$:$10Sb_2O_3$:$10Na_2O$:10CaO :$10Y_2O_3$:$10B_2O_3$:2 Pr_2O_3

YZLAASLBS (UD)—Represents undoped Yttrium Zinc Lithium Alumino Antimony Sodalime Borosilicate glass specimen.
YZLAASLBS (PR) -Represents Pr^{3+} Yttrium Zinc Lithium Alumino Antimony Sodalime Borosilicate glass specimens.

III. THEORY

A. *Oscillator Strength*

The intensity of spectral lines are expressed in terms of oscillator strengths using the relation [19].

$$f_{expt.} = 4.318 \times 10^{-9} \int \varepsilon(\nu)\, d\nu \quad (1)$$

where, $\varepsilon(\nu)$ is molar absorption coefficient at a given energy ν (cm^{-1}), to be evaluated from Beer–Lambert law.

Under Gaussian Approximation, using Beer–Lambert law, the observed oscillator strengths of the absorption bands have been experimentally calculated, using the modified relation [20].

$$P_m = 4.6 \times 10^{-9} \times \frac{1}{cl} \log \frac{I_0}{I} \times \Delta\upsilon_{1/2} \quad (2)$$

where c is the molar concentration of the absorbing ion per unit volume, I is the optical path length, $\log I_0/I$ is absorbtivity or optical density and $\Delta\upsilon_{1/2}$ is half band width.

B. *Judd-Ofelt Intensity Parameters*

According to Judd [21] and Ofelt [22] theory, independently derived expression for the oscillator strength of the induced forced electric dipole transitions between an initial J manifold $|4f^N (S, L) J\rangle$ level and the terminal J' manifold $|4f^N (S',L') J'\rangle$ is given by:

$$\frac{8\Pi^2 mc\bar{\upsilon}}{3h(2J+1)} \frac{1}{n}\left[\frac{(n^2+2)^2}{9}\right] \times S(J, J') \quad (3)$$

where,

the line strength S (J, J') is given by the equation

$$S(J, J') = e^2 \sum \Omega_\lambda \langle 4f^N (S, L) J \| U^{(\lambda)} \| 4f^N (S', L') J' \rangle^2 \quad (4)$$

$\lambda = 2, 4, 6$

In the above equation m is the mass of an electron, c is the velocity of light, ν is the wave number of the transition, h is Planck's constant, n is the refractive index, J and J' are the total angular momentum of the initial and final level respectively, Ω_λ (λ = 2, 4 and 6) are known as Judd-Ofelt intensity parameters.

C. *Radiative Properties*

The Ω_λ parameters obtained using the absorption spectral results have been used to predict radiative properties such as spontaneous emission probability (A) and radiative life time (τ_R), and laser parameters like fluorescence branching ratio (β_R) and stimulated emission cross section (σ_p).

The spontaneous emission probability from initial manifold $|4f^N (S', L') J'\rangle$ to a final manifold $|4f^N (S, L) J\rangle$ is given by:

$$A[(S', L') J'; (S, L) J] = \frac{64\pi^2\nu^3}{3h(2J'+1)}\left[\frac{n(n^2+2)^2}{9}\right] \times S(J', \bar{J}) \quad (5)$$

Where, $S(J', J) = e^2 [\Omega_2 \| U^{(2)} \|^2 + \Omega_4 \| U^{(4)} \|^2 + \Omega_6 \| U^{(6)} \|^2]$

The fluorescence branching ratio for the transitions originating from a specific initial manifold $|4f^N (S', L') J'\rangle$ to a final many fold $|4f^N (S, L) J\rangle$ is given by

$$\beta[(S', L') J'; (S, L) J] = \sum_{S\,L\,J} \frac{A[(S' L')]}{A[(S' L') J' (\bar{S}\ L)]} \quad (6)$$

where, the sum is over all terminal manifolds.

The radiative life time is given by

$$\tau_{rad} = \sum_{S\,L\,J} A[(S', L')\,J'; (S,L)] = A_{Total}^{-1} \quad (7)$$

where, the sum is over all possible terminal manifolds. The stimulated emission cross -section for a transition from an initial manifold $|4f^N (S', L')\,J'>$ to a final manifold $|4f^N (S, L)\,J>|$ is expressed as

$$\sigma_p(\lambda_p) = \left[\frac{\lambda_p^4}{8\pi c n^2 \Delta\lambda_{eff}}\right] \times A[(S', L')\,J'; (\bar{S}, \bar{L})\bar{J}] \quad (8)$$

where, λ_p the peak fluorescence wavelength of the emission band and $\Delta\lambda_{eff}$ is the effective fluorescence line width.

D. Nephelauxetic Ratio (β) and Bonding Parameter ($b^{1/2}$)

The nature of the R-O bond is known by the Nephelauxetic Ratio (β') and Bonding Parameters ($b^{1/2}$), which are computed by using following formulae [23, 24]. The Nephelauxetic Ratio is given by

$$\beta' = \frac{\nu_g}{\nu_a} \quad (9)$$

where, ν_a and ν_g refer to the energies of the corresponding transition in the glass and free ion, respectively. The values of bonding parameter $b^{1/2}$ are given by

$$b^{1/2} = \left[\frac{1-\beta'}{2}\right]^{1/2} \quad (10)$$

IV. RESULT AND DISCUSSION

A. XRD Measurement

Figure 1 presents the XRD pattern of the samples containing show no sharp Bragg's peak, but only a broad diffuse hump around low angle region. This is the clear indication of amorphous nature with in the resolution limit of XRD instrument.

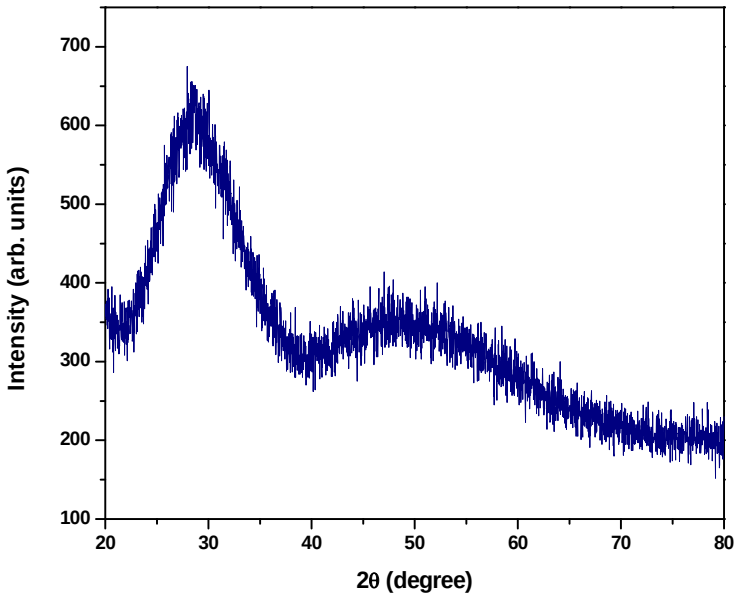

Fig.1: X-ray diffraction pattern of YZLAASLBS PR(1.0) glass.

B. Raman Spectrum

The Raman spectrum of yttrium zinc lithium alumino antimony sodalime borosilicate YZLAASLBS PR(1.0) glass specimen has been presented in Figure 3.The spectrum peaks located at 600,795 and 1205 cm^{-1}.The band at 600 cm^{-1} is assigned to vibrations of Si-O-Si symmetric stretching . The band at 795 cm^{-1} is due to bending vibrations. The bands at 1205 cm^{-1} is due to the Si-O-Si asymmetric stretching.

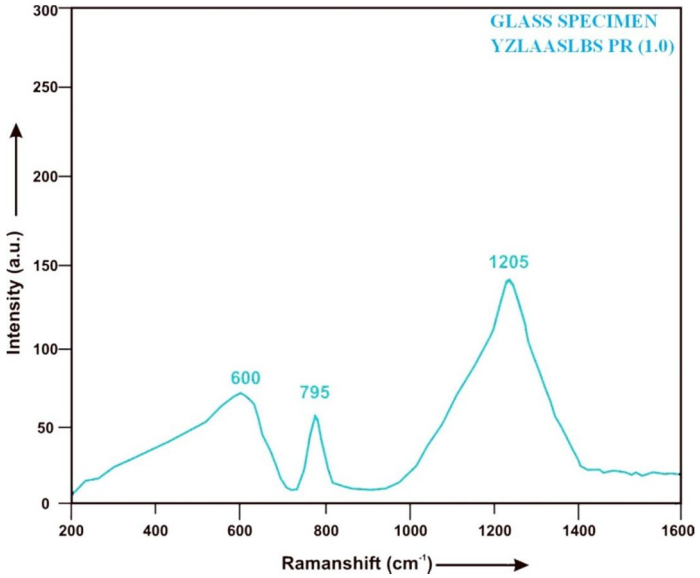

Fig.2: Raman spectrum of YZLAASLBS PR (1.0) glass.

C. Thermal Property

Differential thermal analysis checks the heat absorbed by glass samples during heating or cooling. Fig. 3 depicts the DTA thermogram of powdered YZLAASLBS PR(1.0) sample. The glass transition temperature (T_g), onset crystallization temperature (T_c), crystallization temperature (T_p), melting temperature(T_m), thermal stability (T_s),Balaji Parameter (B_P), Hurbe's criterion (H_R) and reduced glass transition temperature (T_{rg}) were calculated. Shankar's parameter also calculated by using eq. (15). All the determined thermal parameters are given in table 2.

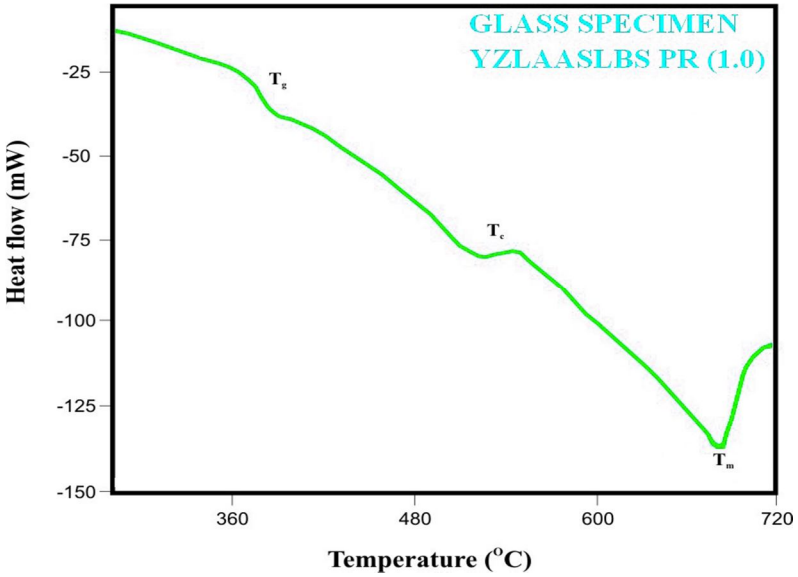

Fig.3: DTA curve of YZLAASLBS PR (1.0) glass.

Table 2. Thermal parameters determined from the DTA traces of YZLAASLBS PR glasses.

Sample Name	T_g(^{0}C)	T_c(^{0}C)	T_p(^{0}C)	T_m(^{0}C)	T_s(^{0}C)	B_P(^{0}C)	H_R(^{0}C)	K_S(^{0}C)	T_{rg}(^{0}C)
YZLAASLBS PR (1.0)	375	508	548	685	133	3.325	0.226	34.366	0.547
YZLAASLBS PR (1.5)	380	510	550	688	130	3.250	0.225	33.634	0.552
YZLAASLBS PR (2.0)	386	513	555	693	127	3.023	0.223	32.987	0.557

The thermal stability of the glass samples can be calculated by difference between onset crystallization temperature and transition temperature [25].

Thermal Stability (T_s)= T_c-T_g (11)

Balaji Parameter can be calculated using [25].

Balaji Parameter (B_P) = [(T_c-T_g)/(T_p-T_c)] (12)

Hruby's criterion is calculated using the Hurby's relation [25].

Hruby's criterion(H_R)=[(T_p-T_c)/(T_m-T_c)] (13)

Reduced glass transition temperature is given as [25].

Reduced glass transition temperature (T_{rg}) =T_g/T_m (14)

Thermal Parameter is given as [25].

K_S= [(T_m-T_c) (T_c-T_g)/T_m] (15)

D. Absorption Spectra

The absorption spectra of YZLAASLBS PR(1.0) glass, consists of absorption bands corresponding to the absorptions from the ground state $^3H_4$ of Pr^{3+} ions. Eight absorption bands have been observed from the ground state $^3H_4$ to excited states $^3F_2$, $^3F_3$, $^3F_4$, $^1G_4$, $^1D_2$, $^3P_0$, $^3P_1$ and $^3P_2$ for Pr^{3+} doped YZLAASLBS PR(1.0) glasses.

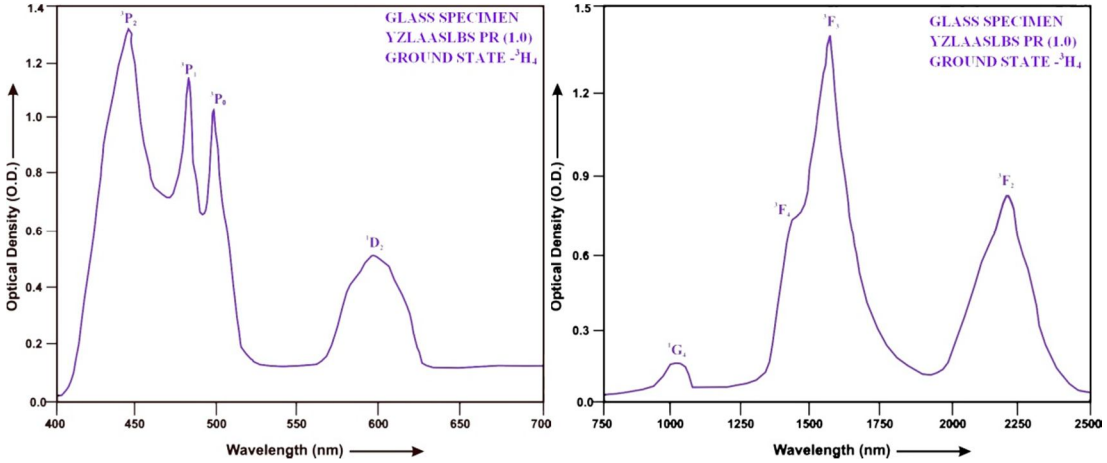

Fig.4: Absorption spectra of YZLAASLBS PR (1.0) glass.

The experimental and calculated oscillator strengths for Pr^{3+} ions in yttrium zinc lithium alumino antimony sodalime borosilicate glasses are given in Table 3

Table 3. Measured and calculated oscillator strength ($P^m \times 10^{+6}$) of Pr^{3+} ions in YZLAASLBS glasses.

Energy level $^3H_4$	Glass YZLAASLBS PR(1.0)		Glass YZLAASLBS PR(1.5)		Glass YZLAASLBS PR(2.0)	
	$P_{exp.}$	$P_{cal.}$	$P_{exp.}$	$P_{cal.}$	$P_{exp.}$	$P_{cal.}$
$^3F_2$	4.55	3.77	3.65	2.92	2.64	2.12
$^3F_3$	6.88	5.98	5.34	4.45	4.64	3.83
$^3F_4$	4.34	3.75	3.49	2.91	2.35	2.37
$^1G_4$	0.45	0.31	0.37	0.24	0.25	0.20
$^1D_2$	2.38	1.06	2.08	0.80	1.64	0.68
$^3P_0$	4.58	1.36	3.68	0.71	2.67	1.02
$^3P_1$	4.78	2.47	3.88	1.45	2.93	1.74
$^3P_2$	12.67	3.55	11.74	2.68	10.59	2.26
R.m.s.deviation	3.5705		3.5350		3.0668	

Computed values of Slater-Condon, Lande′, Racah, nephelauexetic ratio and bonding parameter for Pr^{3+} doped YZLAASLBS glass specimens are given in **Table 4**.

Table4. Computed values of Slater-Condon, Lande′, Racah, nephelauexetic ratio and bonding parameter for Pr^{3+} doped YZLAASLBS glass specimens.

Parameter	Free ion	YZLAASLBS PR(1.0)	YZLAASLBS PR(1.5)	YZLAASLBS PR(2.0)
$F_2(cm^{-1})$	322.09	300.01	300.01	300.02
$F_4(cm^{-1})$	44.46	44.27	44.26	44.27
$F_6(cm^{-1})$	4.867	4.412	4.412	4.412
$\xi_{4f}(cm^{-1})$	741.00	858.41	858.59	858.44
$E^1(cm^{-1})$	4728.92	4450.98	4450.88	4451.20
$E^2(cm^{-1})$	24.75	22.01	22.01	22.01
$E^3(cm^{-1})$	478.10	454.74	454.69	454.73
F_4/F_2	0.13804	0.14755	0.14752	0.14754
F_6/F_2	0.01511	0.01470	0.01471	0.01471
E^1/E^3	9.8911	9.7881	9.7888	9.7887
E^2/E^3	0.0518	0.0484	0.0484	0.484
β'		0.8887	0.8887	0.8887
$b^{1/2}$		0.2359	0.2359	0.2359

The values of Judd-Ofelt intensity parameters are given in Table 5.

Table 5. Judd-Ofelt intensity parameters for Pr^{3+} doped YZLAASLBS glass specimens.

Glass Specimen	$\Omega_2(pm^2)$	$\Omega_4(pm^2)$	$\Omega_6(pm^2)$	Ω_4/Ω_6	Ref.
YZLAASLBS PR(1.0)	3.190	2.121	5.779	0.3670	P.W.
YZLAASLBS PR(1.5)	2.593	1.088	4.522	0.2406	P.W.
YZLAASLBS PR(2.0)	1.443	1.564	3.642	0.4294	P.W.
ZLASVBB (ER)	0.8634	0.3063	0.9618	0.3185	[26].

E. Excitation Spectrum

Excitation spectra of YZLAASLBS PR (1.0) glass recorded at the emission wavelength 395 nm is depicted as figure 5. The excitation spectra consists of three peaks corresponding to the transitions from the ground state $^3H_4$ to the various excited states $^3P_2$, $^3P_1$ and $^3P_0$ at the wavelengths of 448, 465 and 486 nm respectively. Among these, a prominent excitation band at 448 nm has been selected for the measurement of emission spectrum of YZLAASLBS PR (1.0) glass.

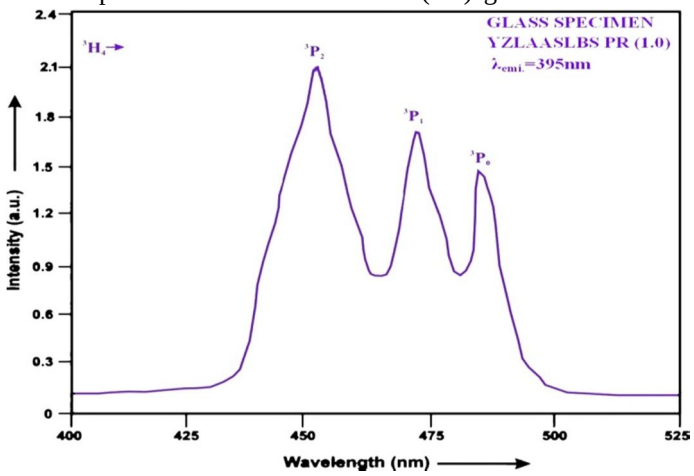

Fig.5: Excitation Spectrum of YZLAASLBS PR (1.0) glass.

F. Fluorescence Spectrum

The fluorescence spectrum of Pr^{3+}doped in ytterium zinc lithium alumino antimony sodalime borosilicate glass is shown in Figure 6. There are nine broad bands ($^3P_0 \rightarrow {}^3H_4$), ($^3P_0 \rightarrow {}^3H_5$), ($^1D_2 \rightarrow {}^3H_4$) ($^3P_0 \rightarrow {}^3H_6$), ($^3P_0 \rightarrow {}^3F_2$), ($^3P_1 \rightarrow {}^3F_3$), ($^1D_2 \rightarrow {}^3H_5$), ($^3P_0 \rightarrow {}^3F_4$) and ($^1G_4 \rightarrow {}^3H_5$) respectively for glass specimens.

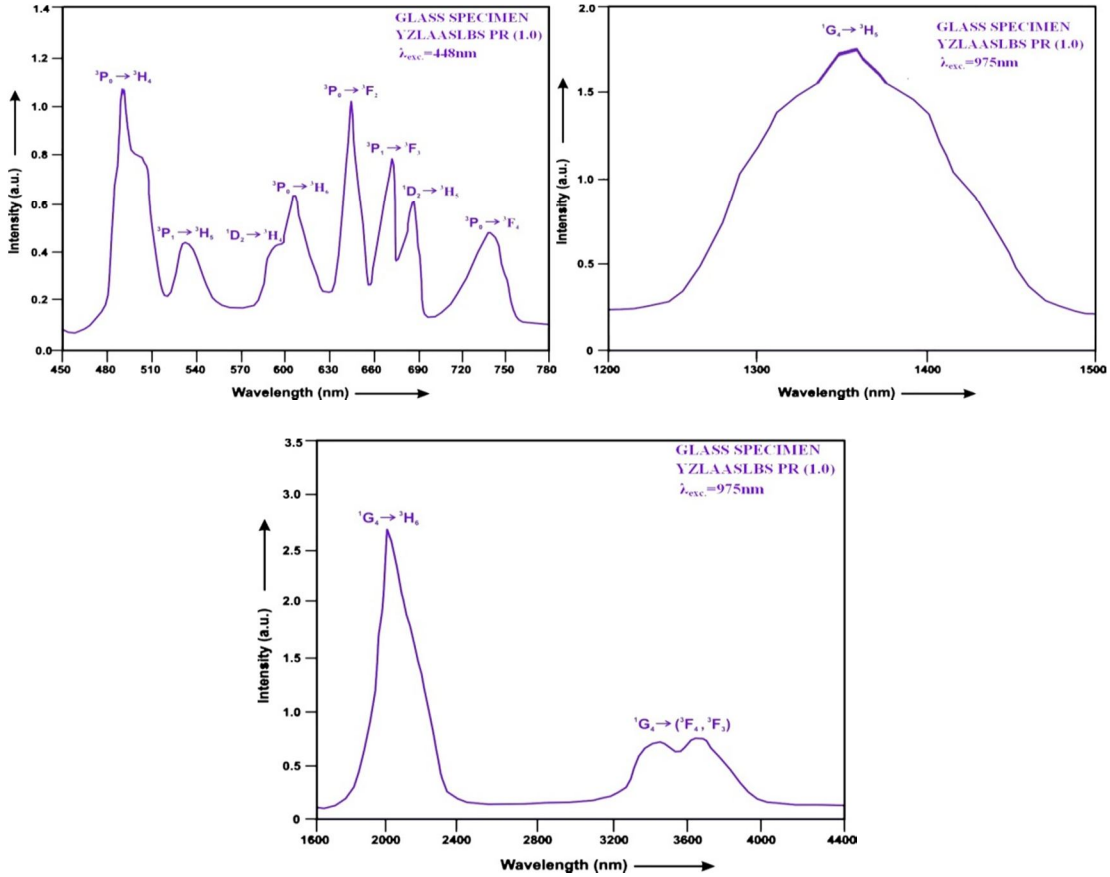

Fig.6: Fluorescence spectrum of YZLAASLBS PR (1.0) glass.

Table 6. Emission peak wave lengths (λ_p), radiative transition probability (A_{rad}), branching ratio (β_R), stimulated emission crosssection (σ_p), and radiative life time (τ) for various transitions in Pr^{3+} doped YZAASLBS glasses.

Transition		YZLAASLBS PR(1.0)				YZAASLBS PR(1.5)				YZAASLBS PR (2.0)			
	λ_{max} (nm)	$A_{rad}(s^{-1})$	β	σ_p (10^{-20} cm^2)	τ_R(μs)	$A_{rad}(s^{-1})$	β	$\sigma_p(10^{-20}$ cm^2)	τ_R (μs)	$A_{rad}(s^{-1})$	β	σ_p (10^{-20} cm^2)	τ_R (10^{-20} cm^2)
$^3P_0 \rightarrow {}^3H_4$	485	1071.84	0.1076	0.366		550.92	0.0772	0.195		793.53	0.1373	0.293	
$^3P_1 \rightarrow {}^3H_5$	529	2051.34	0.2058	0.425		130.90	0.1835	0.275		11417.25	0.2451	0.303	
$^1D_2 \rightarrow {}^3H_4$	599	5109.40	0.0513	0.215		386.11	0.0541	0.166		327.40	0.0566	0.143	
$^3P_0 \rightarrow {}^3H_6$	602	448.08	0.0450	0.248		351.32	0.0493	0.198		283.52	0.0490	0.164	
$^3P_0 \rightarrow {}^3F_2$	645	2138.61	0.2146	2.044		1741.85	0.2442	1.723		971.13	0.1680	0.983	
$^3P_1 \rightarrow {}^3F_3$	676	3136.76	0.3148	1.770		2379.49	0.3336	1.356		1591.58	0.2752	0.922	
$^1D_2 \rightarrow {}^3H_5$	685	5.43	0.0005	0.0061	100.34	1741.85	0.00047	0.0038	140.19	3.809	0.0007	0.0045	172.96
$^3P_0 \rightarrow {}^3F_4$	730	197.99	0.0199	0.155		101.77	0.0142	0.0812		146.58	0.0254	0.119	
$^1G_4 \rightarrow {}^3H_5$	1350	244.22	0.0245	0.875		187.23	0.02624	0.676		154.40	0.0267	0.560	
$^1G_4 \rightarrow {}^3H_6$	2025	141.97	0.0142	5.314		108.17	0.0152	4.121		82.63	0.0143	3.189	
$^1G_4 \rightarrow (^3F_4, {}^3F_2)$	3555	18.56	0.0019	3.502		13.94	0.0020	2.653		9.65	0.0017	1.849	

V. CONCLUSION

In the present study, the glass samples of composition (20-x):SiO_2:10ZnO :10Li_2O :10Al_2O_3 :10Sb_2O_3 :10Na_2O :10CaO :10Y_2O_3 :10B_2O_3:xPr_2O_3 (where x =1, 1.5, 2 mol %) have been prepared by melt-quenching method. Balaji and Shankar parameters indicate that the prepared glass samples have good thermal stability.

The stimulated emission cross-section (σ_p) has highest value for the transition ($^1G_4 \rightarrow {}^3H_6$) in all the glass specimen doped with Pr^{3+}ion. This shows that ($^1G_4 \rightarrow {}^3H_6$) transition is most probable transition and it useful for display device applications.

REFERENCES

[1] Meena,S.L.(2026).Spectral, Thermal and Luminescent Properties of Nd^{3+} Doped Borophosphate Glasses for 1075 nm NIR Photonic broad band Amplification applications,IOSR Appl.Phys.18,16-27.
[2] Sailaja,P.,Mahamuda,Sk.,Dedeepya,G.,Alzahrani,J.S.,Swapna,K.,Venkateswarlu,M.,Rao,A.S.,Alrowaili,Z.A.,Olarinoye,I.O.,Al-Buriahi,M.S.(2024).Effect of Eu^{3+} ions concentration on visible red luminescence and radiative shielding properties of SrO-Al_2O_3-$BaCl_2$-B_2O_3-TeO_2 glasses,Rad.Phys.Chem.216,111467.
[3] Rani,P.R.,Venkateswarlu,M.,Mahamuda,S.,Swapna,K.,Deopa,N.,Rao,A.S.,Prakash,G.V.(2019).Structural,absorption and photoluminescence studies Sm^{3+} ions doped barium lead fluoroborate glasses for optoelectronic device applications. Mat. Reasearch Bulletin,110, 159-168.
[4] Meena,S.L.(2024).Spectral and Thermal properties of Tm^{3+} doped in Zinc Lithium Tungsten Alumino Phosphate glasses,IOSR Appl.Phys.16,64-75
[5] Meena,S.L.(2026).Spectral, Transmittance and Thermal Analysis of Tb^{3+} doped Ytterbium Zinc Lithium Calcium Borogerminate Glasses,IOSR,Appl.Phys.18,31-38.
[6] Wang,M.T.,Cheng,J.S.,Li,M.,He,F.(2011).Structure and properties of sodalime silicate glass doped with rare earth.Phys.B Condens.Matter,406,187-191.
[7] Zhao,G.Y.,Tian,Y.,Wang,X.,Fan,H.Y.,Hu,L.L.(2013).Spectroscopicproperties of 1.08µm emission in Tm^{3+} doped bismuth silicate glass,J.Lumin.134,837-841.
[8] Babu,K.V.,Cole,S.(2018).Luminescence properties of Dy^{3+} doped alkali lead alumino borosilicate glasses,Ceram.Int.9080-9090.
[9] Cao,W.,Huang,F.,Wang,T.,Ye,R.,Lei,R.,Tian,Y.,Zhang,J.,Xu,S.(2018).2.0µm emission of Ho^{3+} doped germanosilicate glass sensitized by non-rare earth ion Bi: a new choice for 2.0 µm laser,Opt.Mater,75,695-698.
[10] Monisha, M., Nancy,A. , Souza, D., Nimitha ,V. L., Prabhu, S and Sayyed, M.I.(2020). Dy^{3+} doped SiO_2- B_2O_3-Al_2O_3-NaF-ZnF_2 glasses: An exploration of optical and gamma radiation shielding features, Current Applied Physics 20(11), 1207-1210.
[11] Sroda,M.,Swiontek,S.,Gieszczyk,W.,Bilski,P.(2020).The effect of lithium fluoride on the thermal stability and thermoluminescence properties of borosilicate glass and glass ceramics,J.Eur,Ceram.Soc.40,472-479.
[12] Mi-tang Wang , Jin-shu Cheng, Mei Li and Feng He(2011). Structure and properties of soda lime silicate glass doped with rare earth. Physica B 406, 187–191.
[13] Tian,C.,Chen,Xi,Shuibao,Yu(2015).Concentration dependence of spectroscopic properties and energy transfer analysis in Nd^{3+} doped bismuth silicate glasses,Solid State Sci.48,171-176.
[14] Meena,S.L.(2021).Spectral and Raman Analysis of Sm^{3+} doped in Zinc Lithium Sodalime Alumino Silicate Glasses,Int.J.Eng.Sci.Inven.10,28-33.
[15] Yasukevich,A.S.,Dunia,G.,Kisel,V.E.E.,Kuleshov,N.V.(2020).Spectralluminescence properties of oxyfluoride lead silicate germinate.J.Lumin.229,117667.
[16] Meena,S.L.(2025).Spectral, Thermal and Raman Analysis of Dy^{3+} Doped Borosilicate Glasses with Large Thermal Stability Parameter, Int.J.Eng.Sci.Inv.14,11-18.
[17] Matos,I.M.,Balzaretti, N.M.(2024).Effect of mixed alkali ions on the structural and spectroscopic properties of Nd^{3+} doped silicate glasses,Res.Mat.21,100517,1-8.
[18] Meena,S.L.(2020).Judd-Ofelt analysis of Gd^{3+} Doped in Lead Lithium Antimony Alumino Sodalime Silicate Glasses, Int.J.Chem.Phy.Sci.9,13-22.
[19] Meena,S.L.(2021). Spectral and Thermal properties of Pr^{3+} doped lead lithium sodium tungsten borophosphate glasses,IOSR Appl.Phys.13,1-7.
[20] Meena,S.L.(2021). Spectral and Raman Analysis of Er^{3+} doped Zinc Lithium Antimony Sodalime Tellurite Glasses,Int.J.Eng.Sci.Inv.10,09-15.
[21] Judd, B.R. (1962). Optical Absorption Intensities of Rare Earth Ions. Physical Review, 127, 750.
[22] Ofelt, G.S. (1962). Intensities of Crystal Spectra of Rare Earth Ions. The J. Chem. Phys., 37, 511.
[23] Sinha, S.P. (1983). Systematics and properties of lanthanides, Reidel, Dordrecht.
[24] Krupke, W.F. (1974).IEEE J. Quantum Electron QE, 10,450.
[25] Meena,S.L.(2026). Spectral,Thermal and Luminescent properties of Nd^{3+} doped borophosphate glasses for 1075µm NIR Photonic broad band Amplification applications, glasses, IOSR Appl.Phys.18,16-23.
[26] Meena,S.L.(2024).Spectral and Luminescence Study of Er^{3+} doped Phosphate Glasses for the Development of 1.5 µm Broadband Amplifier,IOSR Appl.Phys.16,35-41.

ISSN: 2321-9653; IC Value: 45.98; SJ Impact Factor: 7.538
Volume 14 Issue VI June 2026- Available at www.ijraset.com

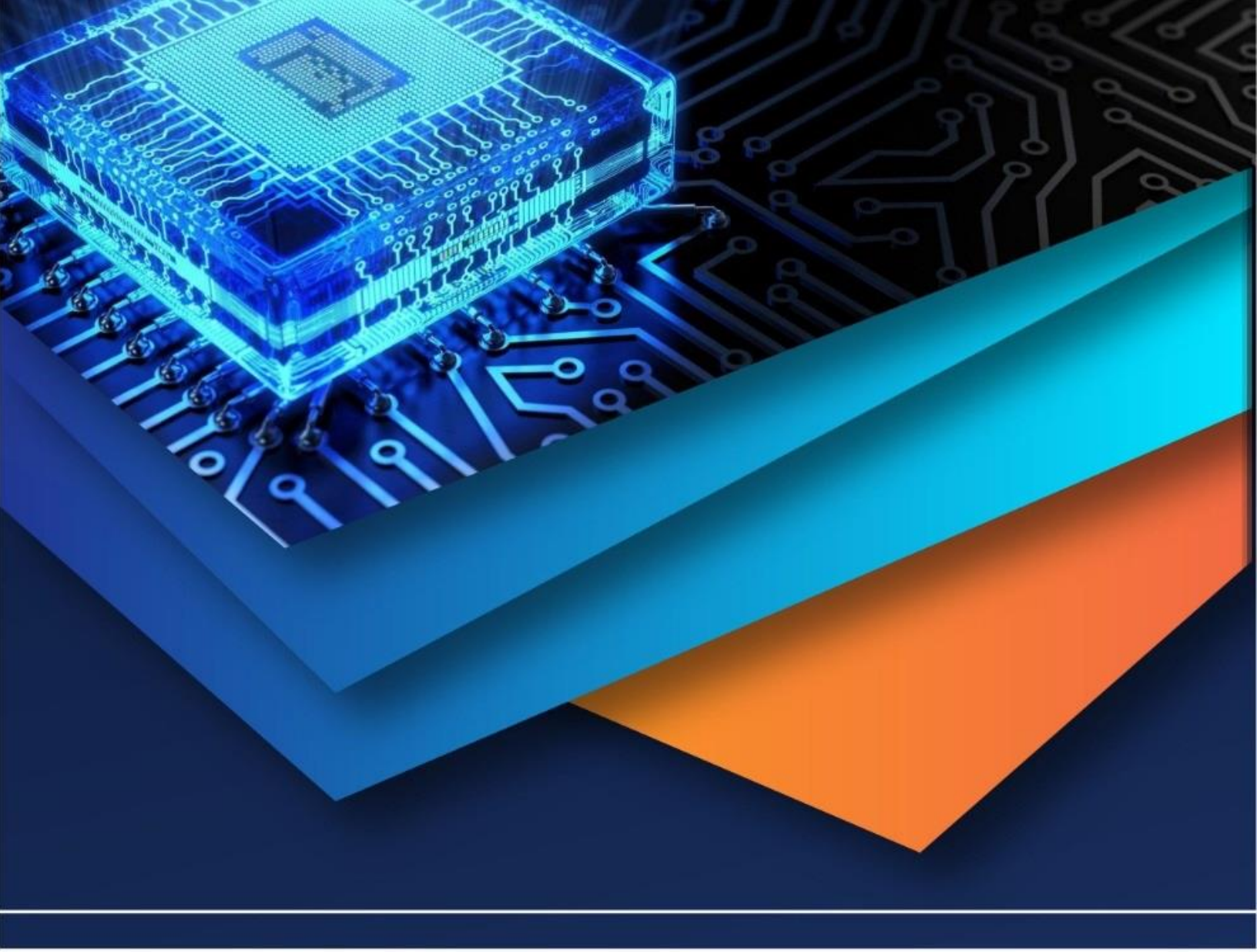

10.22214/IJRASET

45.98

IMPACT FACTOR: 7.129

IMPACT FACTOR: 7.429

INTERNATIONAL JOURNAL FOR RESEARCH

IN APPLIED SCIENCE & ENGINEERING TECHNOLOGY